Seepage through earth dams with horizontal filters and founded on impervious foundation (numerical analysis with boundary element method)

Hossam A. Abdel-Gawad and Mohamed T. Shamaa
Irrigation and Hydraulic Eng. Dept., Faculty of Eng. Mansoura University, Mansoura , Egypt

In this research, the Boundary Element Method (BEM) was applied for Laplace's equation to solve the problem of seepage through earth dams underlined by horizontal filter. Linear elements were used to discretize the boundary of the flow domain. A novel idea was used to assure convergence of the unknown free surface to the correct one. Also, the effects of local singularity and numerical/analytical integration on the global solution were tested. The numerical results have an excellent agreement with the analytical/exact solutions.

في هذا البحث طبقت طريقة العناصر المحيطة علي معادلة لابلاس لحل مشكلة السريان خلال السدود الترابية المزودة بمرشح أفقي. وقد استخدمت العناصر الخطية لتمثيل حدود مجال السريان. هذا وقد طبقت فكرة جديدة لضمان تقارب سطح المياه المحسوب لمكانة الحقيقي. كما تم دراسة تأثير تواجد حل مفرد عند بعض النقاط وتأثير استخدام متكاملات عددية أو تحليلية على الحل العام. وقد أعطت الحلول العددية توافق ممتاز مع الحلول التحليلية.

Keywords: Earth dam, Horizontal filter, Unconfined seepage, Boundary element method Singularity, Numerical/Analytical Integration

1. Introduction

This work focused on trapezoidal earth dams provided with horizontal filters. Determining the position of seepage surface and its exit point with the filter is a necessary step to complete the design procedure of the dam. Kozeny [1], using conformal mapping, studied this problem for dams with parabolic upstream faces resting on an impervious base. He concluded that the phreatic surface has a parabolic shape. Later, Cassgrande in [2] suggested an approximation to make Kozeny's solution available to simulate the seepage line through earth dam with trapezoidal cross section [1]. Using a modified form of Zhukovsky's function Nelson-Skornyakov [1] obtained exact solutions for two relatively simple cases, a dam with horizontal upstream slope and another one with approximately vertical upstream face. The dam is resting on homogenous foundation of infinite depth. Moayeri [2] obtained the most accurate analytical solution for seepage through trapezoidal dams taking in account the effect of the inflection point on the free surface. He used inverse hodograph and conformal mapping. Hathoot [3] solved the problem using the image theory. He constructed his analyses on unrealistic assumptions: 1) flow leave the dam through the whole length of the horizontal filter, 2) uniform rates of seepage along the upstream face and the downstream filter of the dam, 3) equation used to simulate seepage through the wetted part of the upstream face of the dam were settled in unsatisfactory formulation, that it simulated a uniform flow through the whole infinite plane above the impervious bed. Wrong stream function Ψ was concluded. Using that function along the filter, zero value of Ψ was always calculated. Due to the previous assumptions Hathoot's results were found far from analytical results according to Numerov [1].

With the increase developments of the computer systems numerical methods started to handle the present problem. The main disadvantages of the numerical solutions are the bad convergence of the solution besides the existing of oscillations along the free surface when approaches vertical or near vertical. To eliminate these disadvantages, Neuman [4] combined the regular Finite Element Method (FEM) with a minimization function for the difference between inflow and outflow seepage through the dam.

Liggett [5] used the Boundary Element Method (BEM) to solve the problem of unsteady seepage through earth dams without drains starting from known initial location of the free surface. Cabral [6] developed a new BEM formulation using cubic B-splines, which provides continuity till the second derivative of the potential head. Also, he studied only dams without drains. Abdrabbo [7] studied the present problem using the BEM with constant elements. He simplified the problem by suggesting in advance different positions for the exit point of the free surface with the drain. To the author knowledge there is no previous trial to analysis our problem that is determining the location of the free surface and its exact exit point, using the BEM. This is may be due to the appearance of more accurate and stable philosophy that adopted the effect of the partially saturated zone above the free surface [8, 9]. This philosophy that is more logic based on Richard's equation and a specified relation between pore water pressure and hydraulic conductivity. The aforementioned disadvantages, when handling Laplace's equation with numerical methods, eliminated through this approach. It must be noticed that, there is no fundamental equation for Richard's equation, thus BEM is not applicable for that equation.

The principle purpose of the present study is to make use of the BEM to obtain a numerical solution for the problem of seepage through homogeneous isotropic earth dams with horizontal filters and resting on impervious foundations. Also, the effects of singularity and integration process on accuracy of the solution were taken into consideration.

2. Theoretical background

The vertical two-dimensional steady incompressible laminar flow through a saturated homogenous anisotropic earth dam is governed by Harr [1]:

$$\frac{\partial}{\partial x}\left[k_x \frac{\partial \varphi}{\partial x}\right] + \frac{\partial}{\partial y}\left[k_y \frac{\partial \varphi}{\partial y}\right] = 0.0 \,. \qquad (1)$$

Assuming isotropic hydraulic conductivity with constant value reduces eq. (1) to the following Laplace's equation:

$$\frac{\partial^2 \varphi}{\partial x^2} + \frac{\partial^2 \varphi}{\partial y^2} = 0.0 \,, \quad \varphi(x,y) = \frac{p(x,y)}{\rho g} + y \,, \qquad (2)$$

where φ is the potential head (L), p is the excess pore water pressure (F/L^2), ρ is the water density (M/L^3), g is the acceleration due to gravity (L/T^2), (k_x, k_y) are hydraulic conductivities in (x, y) directions (L/T), and y is the elevation above the impervious bed of the dam (L). For the dam studied in fig. 1 the boundary condition are:

$\varphi = Hu$ on AB [Dirichlet B.C.] (3-a)

$q_n = k\frac{\partial \varphi}{\partial n} = 0.0$ on BC [Neumann B.C.], (3-b)

$\varphi = 0.0$ on CD [DirichletB.C.], (3-c)

$q_n = k\frac{\partial \varphi}{\partial n} = 0.0$ & $\varphi = y$ on DA [*Neumann & Dirichlet B.C.'s*] (3-d)

where, Hu is the upstream water head (L), $\partial/\partial n$ the derivative with respect to the normal ($1/L$), q_n is the normal seepage (L/T), and k is the hydraulic conductivity (L/T). The location of the free surface and its exit point D are unknowns in advance, so the problem is nonlinear and must be solved through iteration process starting from an initial guess.

3. Boundary element method

In this numerical method, only boundary of the problem must be discretized with nodes in counterclockwise numbering. This reduces the dimensionality of the problem by one. Linear elements were adopted to simulate the boundary by attaching every two consecutive nodes. This means that, through any element both of φ and q are represented by line connecting their values at the extreme nodes.

This is the only approximation considered when applying BEM. The effect of this approximation vanishes with increasing number of nodes discretizing the problem boundary. On essential condition to apply BEM to any problem is the existing of a fundamental solution for its governed equation. The fundamental solution ψ for Laplace's equation is [10]:

$$\nabla^2\psi = -\delta(r) \;\&\quad \psi = (1/2\pi).\ln(1/r), \tag{4}$$

where, r is the distance between any point through the flow domain and any node on the boundary (L), ∇^2 means second derivative, and $\delta(r)$ is the Dirac delta function equals to one only if $r=0.0$, otherwise equals zero. The mathematical basis stems from Green's theorem [10]:

$$\iint_D \left(\varphi\nabla^2\psi - \psi\nabla^2\varphi\right)dxdy = \int_S \left(\varphi\frac{\partial\psi}{\partial n} - \psi\frac{\partial\varphi}{\partial n}\right)ds\,. \tag{5}$$

where, $\iint_D$ means double integration through the flow domain D, $\int_S$ is line integration around the boundary S of flow domain. Eq. (5) can be represented in the following form:

$$c.\varphi(U) = \int_S \left[\varphi(V)\frac{\partial(\ln r)}{\partial n} - \ln r\,\frac{\partial\varphi(V)}{\partial n}\right]dS\,, \tag{6}$$

where, U is any node on the boundary or inside the domain, V is a series of nodes on the boundary over which the integration is performed, c is a constant called the free term equal to 2π if U lies inside the domain, and equal to the interior angle of the boundary in radians if U is located at a node on S. If φ and $\partial\varphi/\partial n$ are known everywhere on the boundary eq. (6) can be directly determined the amount of φ at any interior point through the flow domain. In fact either φ or $\partial\varphi/\partial n$ are given at each boundary node. Thus eq. (6) must be used first to find the missing data by choosing U to be located at a succession of boundary nodes. This creates number of equations N equal to the number of nodes discretize the domain boundary in equivalent number of unknowns at these nodes (φ or $\partial\varphi/\partial n$). These equations can be settled in matrix form as [10]:

$$\{[C]_{N*N} + [E]_{N*N}\}.[\varphi]_{N*1} = [F]_{N*N}.[\partial\varphi/\partial n]_{N*1}, \tag{7}$$

where, $[E]_{N*N}, [F]_{N*N}$ are square coefficient matrices with N rows, $[\varphi]_{N*1}, [\partial\varphi/\partial n]_{N*1}$ are two vectors with N rows, and $[C]_{N*N}$ is a diagonal matrix represents the free terms. Sub-elements in previous matrices can be calculated numerically using Gauss integration as follows, see fig. 2.

$$E_{ij} = G_1^j + G_2^{j-1},\; F_{ij} = A_1^j + A_2^{j-1}, \tag{8}$$

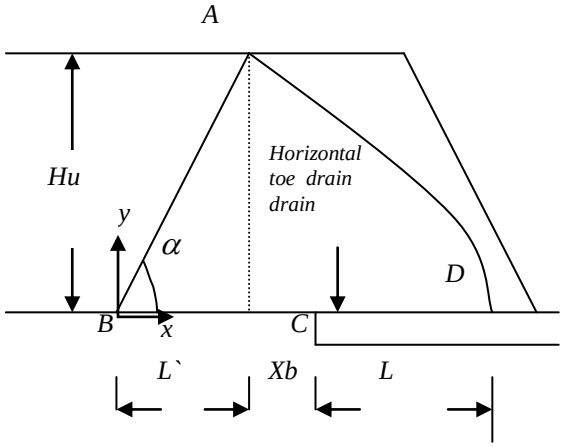

Fig.1. Trapezoidal earth dam with horizontal filter.

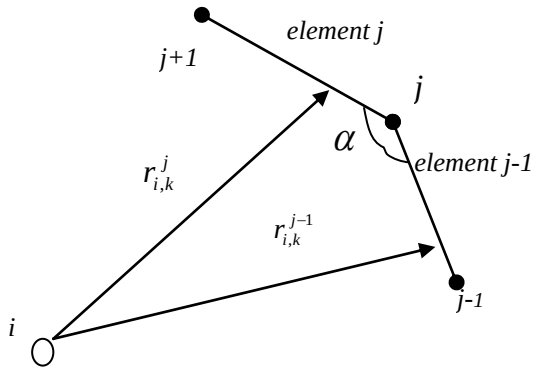

Fig. 2. Notation for a Gauss numerical integration scheme.

where,

$$G_1^j = \frac{L_j}{4}\sum_{k=1}^{M}(\zeta_k - 1)\frac{D_i^j}{\left(r_{i,k}^j\right)^2}\omega_k\ , \tag{9}$$

$$G_2^{j-1} = -\frac{L_{j-1}}{4}\sum_{k=1}^{M}(\zeta_k + 1)\frac{D_i^{j-1}}{\left(r_{i,k}^{j-1}\right)^2}\omega_k\ , \tag{10}$$

$$A_1^j = -\frac{L_j}{4}\sum_{j\ k=1}^{M}(\zeta_k - 1)ln\frac{1}{r_{i,k}^j}\omega_k\ , \tag{11}$$

$$A_2^{j-1} = \frac{L_{j-1}}{4}\sum_{k=1}^{M}(\zeta_k + 1)ln\frac{1}{r_{i,k}^{j-1}}\omega_k\ , \tag{12}$$

$$C_{ii} = -\sum_{j=1}^{j=N}E_{ij} = -\frac{\alpha^o}{180}\pi\ , \tag{13}$$

$$r_{i,k}^j = \sqrt{\left(x_{i,k}^j - x_i\right)^2 + \left(y_{i,k}^j - y_i\right)^2}\ , \tag{14}$$

$$x_{i,k}^j = \left(x_{j+1} + x_j\right)/2 + \zeta_k.(x_{j+1} - x_j)/2\ , \tag{15}$$

$$y_{i,k}^j = \left(y_{j+1} + y_j\right)/2 + \zeta_k.(y_{j+1} - y_j)/2\ , \tag{16}$$

$$D_i^j = 2\left|Ay^j.\left(x_i - x_j\right) - Ax^j.\left(y_i - y_j\right)\right|/L_j\ , \text{ and} \tag{17}$$

$$Ax^j = \left(x_{j+1} - x_j\right)/2\ ,\ Ay^j = \left(y_{j+1} - y_j\right)/2\ , \tag{18}$$

where, L_o represents the length of element *o*, D_i^o is the perpendicular length from node *i* on element *o*, *M* is number of Gauss points which have relative positions ζ_k form 1 to –1 along the studied element and corresponding weights ω_k, α is the interior angle in degrees at node *i*, and $r_{i,k}^o$ is the distance between point *i* and Gauss point *k* along element *o*. To compute $r_{i,k}^{j-1}, D_i^{j-1}$ replace the superscript *j* by *j-1* through eqs. (14-18). If $|i-j| \le 1$ then:

$$F_{i,i-1} = \frac{L_{i-1}}{4}\left(1 + 2\,ln\frac{1}{L_{i-1}}\right) + A_2^{j-2}\ . \tag{19-a}$$

$$F_{i,i} = \frac{L_i}{4}\left(3 + 2\,ln\frac{1}{L_i}\right) + \frac{L_{i-1}}{4}\left(3 + 2\,ln\frac{1}{L_{i-1}}\right), \tag{19-b}$$

$$F_{i,i+1} = -A_1^{j+1} + \frac{L_i}{4}\left(1 + 2\,ln\frac{1}{L_i}\right). \tag{19-c}$$

Matrices in eq. (7) must be rearranged that leads to *N* equations in *N* unknowns (φ or $\partial\varphi/\partial n$).

4. Solution steps

Fortran program BETIS [10], which concerns only with confined/linear flow problems, was modified to be applicable to unconfined/ nonlinear problems. A new procedure for the iteration process was created to assure stability and convergence of the solution. The solution procedure and addend modifications are illustrated in the following steps:

1. Assume initial guess for the crossed part of the horizontal filter. Different equations were tested. The following empirical (suggested) equation was found reasonable, see fig. 1.

$$L = \left[\sqrt{Hu^2 + (L'+Xb)^2} - (L'+Xb)\right]/6.0\ . \tag{20}$$

2. To remove non-linearity from the problem, the unknown free surface is assumed as a straight line with zero normal flow (Neumann B.C.). Then discretize the triangular flow domain with the selected number of nodes. To enhance the solution accuracy, the ratio between any two consequent elements is limited by 0.66 and 1.5. Also, the minimum initial number of nodes simulating the free surface is chosen to be more than 35. Previous constraints increase the convergence speed, catch the curved configuration of the free surface and diminish the difference between seepage flow in and out from the dam.

3. The program BETIS is used to calculate the unknown potential heads for the assumed free surface *AD,* see fig. 1. The free surface is simulated by straight line only at first iteration and be curved as iteration process. Program BETIS uses numerical/Gauss integration to built matrices in eq. (7).

4. After several trials, the polar at point *o* was selected empirically, as shown in fig. 3, with coordinates *xo = Minimum* [*(L`-Hu), L`/2*], *yo =-1.5Hu* and the nodes on the free surface is

moved for the next iteration along the rays connecting the polar *o* and different nodes on *AD*. This alleviates distortion of the ratio between consequent elements on the free surface. Consequently, better representation for the free surface can be achieved.

5. To assure convergence of the problem, nodes representing iterated free surface should not settled outside the actual seepage domain. The iteration process is always started from an underestimated position of the free surface. This produces an overestimated values for the pressure head, consequently the adaptive new free surface will be found higher than the actual one. Therefore, the movements of free surface nodes along their conjunction rays should be limited with only quarter of the differences between calculated potential heads and their vertical elevations. If the elevation of node 2 (as shown in fig. 3) after updating the free surface is more than *0.025* upstream head, add extra nodes to assure this condition, (fig. 3). This enable more accurate representation of the free surface when approaches vertical. Exit point at node 1 must always lies along the filter with *x*-coordinate ≥ *x*-coordinates for node 2. After updating the position of the exit point, rearrange nodes along the filter length to maintain the same ratio between the elements.

6. Recall program BETIS and determine the new values of the potential heads along the free surface. If the maximum difference between the calculated technique used for free surface computation. φ and the elevation head for any node on the free surface greater than $0.0001Hu$ go to step 5, otherwise stop iteration. Maximum allowed number of iterations equal to 500. The solution is called convergent if it stopped in less than 500 iterations.

7. Calculate the total amount of seepage flow in and out the dam.

5. Effect of local singularity

Under certain combinations of geometry and boundary conditions, the solution of Laplace's equation with BEM may include singularity, that the flux reaches infinity at some nodes [10]. One of the most popular

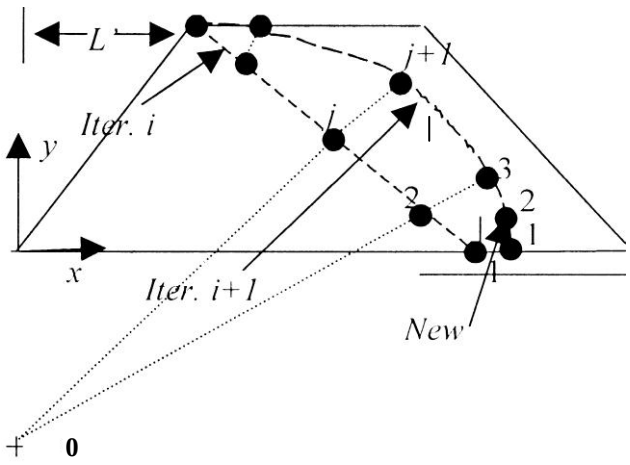

Fig. 3. Solution domain and iteration.

cases is shown in fig. 4, where the potential is known along one side *ON* and the flux is zero along the other side *OM* of the corner with internal angle $\alpha \geq \pi/2$. Motz gave the analytical solution near singular corner *O,* as referenced in [10]. Local flux along the side *ON* is obtained by substituting $\theta = -\alpha/2$ in Motz's solution, then.

$$q = B_1 r^{\gamma-1} + B_2 r^{3\gamma-1} + B_3 r^{5\gamma-1} + .. + B_\infty r^{\infty}, \qquad (21)$$

where, q is the flux at distance r from the singular point *O* along the singular element *ON* with infinity flux at node *O*, $\gamma = \pi/(2\alpha)$, and $B_{1to\infty}$ are unknown constants. The order of singularity is represented by $1-\gamma$. Thus singularity disappears as $\alpha \leq \pi/2$. Coefficient B_1 represents the intensity of the singularity. Number of terms that can be taken into account depends on number of nodes of the singular element. In this work two nodes, similar to the linear element, was taken to represent the singular element. Flux along singular element *ON* can be represented as [10].

$$q(\zeta) = B_1 N_1(\zeta) + q_N N_2(\zeta) \quad , \qquad (22)$$

where,

$$N_2(\zeta) = \left(\frac{1+\zeta}{2}\right)^{3\gamma-1} . \qquad (23)$$

$$N_1(\zeta) = \left(\frac{1+\zeta}{2}\right)^{\gamma-1}\left[1-\left(\frac{1+\zeta}{2}\right)^{2\gamma}\right] L_O^{\gamma-1}, \qquad (24)$$

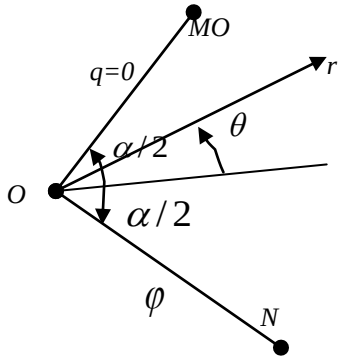

Fig. 4. Local definition of geometry and boundary conditions at singular point O.

where, $q(\zeta)$ represents the flux along the singular element for values of ζ varies form -1 at singular node *O* to +1 for node *N*, q_N is the unknown flux at node *N*, L_o is length of element *ON*. In this work, BETIS was modified that enable replacing any linear element with singular one. Only first element along the filter *CD* fig. 1 was simulated by a singular element to check the effect of local singularity produced from existing zero and infinity fluxes around the two sides of point *C*. The remaining part of the flow boundary was simulated with linear elements. If the singular point coincides with node *j* then [10].

$$F_{i\neq j}=\frac{L_j}{2}\left[\sum_{k=1}^{M}N_1(\zeta)ln\frac{r_{i,j}^{j}}{r_{i,k}^{j}}\omega_k+\frac{4}{3\gamma}L_j^{\gamma-1}ln\frac{1}{r_{i,j}^{j}}\right]. \quad (25)$$

$$F_{i\neq j+1}=A_1^{j+1}+\frac{L_j}{2}\left[\sum_{k=1}^{M}N_2(\zeta)ln\frac{r_{i,j}^{j}}{r_{i,k}^{j}}\omega_k+\frac{2}{3\gamma}ln\frac{1}{r_{i,j}^{j}}\right]. \quad (26)$$

and

$$F_{j,j}=-L_j^{\gamma}\left(\frac{2}{3\gamma}lnL_j-\frac{8}{9\gamma^2}\right). \quad (27)$$

$$F_{j+1,j+1}=A_1^{j+1}-L_j\left(\frac{1}{3\gamma}lnL_j-\frac{1}{9\gamma^2}\right). \quad (28)$$

In case of using singular element the solution retains with the value of B_1 instead of the infinite flux at the singular node. Hence, the flux along the singular element can be determined using eq. (22). The effect of using only linear elements to discretize the domain boundary and replacing first linear element at the outset of the filter with singular element is shown in fig. 5 for a dam has upstream face inclination with horizontal equal to 40°.

Negative seepage values mean that water flows out of the dam. It can be observed that as soon as we approach the singular node at point *C*, the use of linear element at that node produces wrong results that are reflected in jumps in the line joining the nodal results. While using singular element at point *C* eliminates these oscillations, both of total amount of seepage and the position of the free surface are the same for the two cases. This means that using singular element only enhance the local solution around the singular point, whereas the global solution is not affected by this local singularity. Relative seepage rate *q/k* equal to 1.0 at exit point *D*, satisfies the perpendicularity condition of the free surface with the filter.

Analytical solutions always restrict the free surface to be perpendicular on the upstream face of the dam at point *A*, see fig. 1, [1]. For $\alpha<90^{\circ}$ the free surface adjacent to point *A* has a concave configuration. Simulating this part of the free surface by linear element increases the interior angle at point *A* over 90° which distorts the mathematical solution with unreal singularity at point *A*. The exact quantity of the flux at *A* must be equal to $-k.\partial\phi/\partial S = -k.\partial y/\partial S = -k.\sin(\alpha-90)$ [7], where *S* represents distance along the free surface. If the calculated seepage rate at point *A* deviated

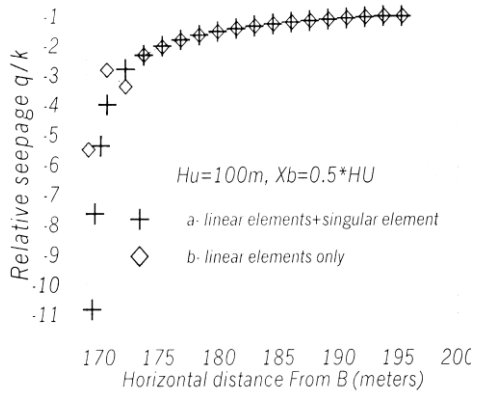

Fig. 5. Effect of replacement first linear element simulates the drain with singular one on the calculated seepage.

from the analytical/exact one, larger number of nodes reused to discritize the domain boundary. This enhances the representation of the free surface, and consequently numerical results of seepage rate at point *A* approaches the exact values.

At the upstream face toe, point *B* in fig. 1, the analytical/exact value for the flux must be always equal to zero for $\alpha < 90^\circ$. In contrast to the exact solution using linear element to simulate this part produces nonzero flux at point *B*, for values of α close to 90°. Thus for the next runs, singular element was used to simulate the lowest part of the upstream face that guarantee existing of zero flux at point *B* for $\alpha < 90^\circ$.

6. Effect of numerical integration

Program BETIS uses only numerical integration to construct matrices in eq. (7). The program was developed to use numerical or analytical integration. The following equations represent different analytical integrands used in eq. (7), [11], see fig. 6.

$$E_{ij} = \frac{-I11_i^j + \xi_i^{j+1} I12_i^j}{L_j} + \frac{I11_i^{j+1} - \xi_i^{j+2} I12_i^{j+1}}{L_{j+1}}, \qquad (29)$$

$$F_{ij} = \frac{-I21_i^j + \xi_i^{j+1} I22_i^j}{L_j} + \frac{I21_i^{j+1} - \xi_i^{j+2} I22_i^{j+1}}{L_{j+1}}, \qquad (30)$$

where, $I11_i^o = D_i^o \ln(r_i^{o+1} / r_i^o)$, (31)

$$I12_i^o = \tan^{-1}(r_i^{o+1}) - \tan^{-1}(r_i^o), \qquad (32)$$

$$I21_i^o = \left\{ r_i^{o+1}\left(2\ln r_i^{o+1} - 1\right) - r_i^o\left(2\ln r_i^o - 1\right)\right\}/4, \qquad (33)$$

$$I22_i^o = \begin{Bmatrix} r_i^{o+1}\ln r_i^{o+1} - r_i^o \ln r_i^o - 2L_o + \\ 2D_i^o\left\{\tan^{-1}(r_i^{o+1}) - \tan^{-1}(r_i^o)\right\} \end{Bmatrix} / 2, \qquad (34)$$

$$\xi_i^o = \sqrt{(r_i^o)^2 - (D_i^o)^2}. \qquad (35)$$

Free surface through a dam with α = 40° was calculated using both of numerical integration with variable number of Gauss points (2 and 4) and analytical integration, as shown in fig. 7. It can be noticed that the obtained free surface is the same for all cases. This means that using numerical integration will give exact values for the integrands even if we use only two Gauss points.

7. Model verification

To check accuracy of the modified mathematical BEM model, the obtained numerical results were compared with both the analytical solutions of Moayeri and Numerov [2] and the approximate solution of Casagrande [1]. Fig. 8 shows comparison between the relative length of the filter *L/Hu* and relative total amount of seepage *Q/(k.Hu)* for different values of $\alpha = 30^\circ, 60^\circ, 90^\circ$. It can be seen that, Casagrande's solutions always underestimate both of *L/Hu* and *Q/(k.Hu)* with respect to both of analytical and BEM solutions. Also it can be noticed that the

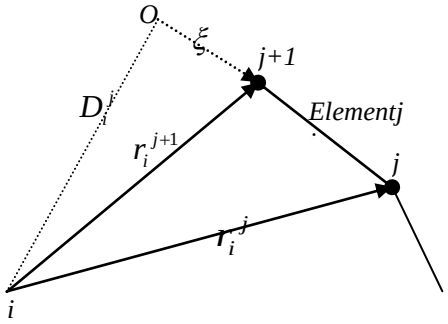

Fig. 6. The $\xi - D$ coordinate system.

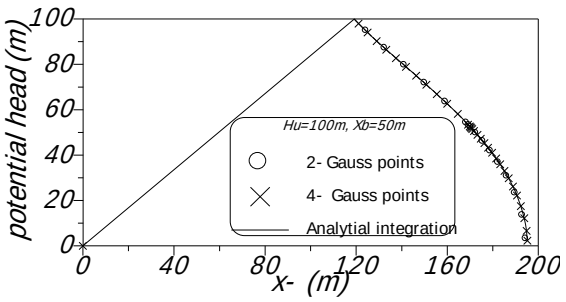

Fig.7. Position of calculated free surface using numerical and analytical integration.

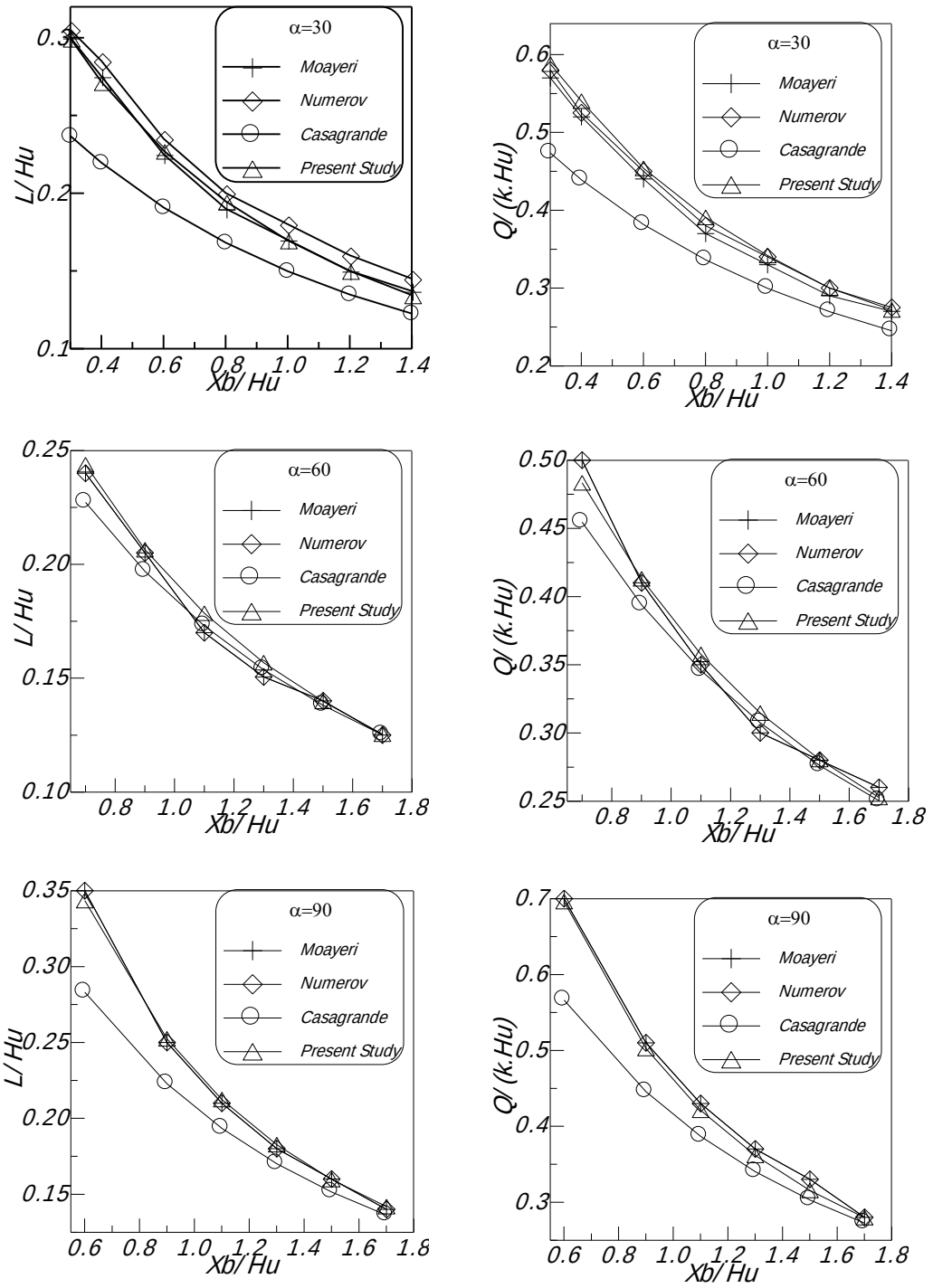

Fig. 8. Comparison between different results of *L/Hu,Q/(k*Hu) u*sing different methods (BEM, Moyeri, Numerov, and Casagrande) for ($\alpha = 30^{\circ}, 60^{\circ}, 90^{\circ}$).

accuracy of Casagrand's approximation decreases as *Xb/Hu* decreases.

In the other hand the analytical solutions of Moyeri and Numerov are in a good agreement with the present BEM results for α=90. As α, decreases there are insignificant discrepancies <5% between analytical and BEM results. In general, BEM results are more close to Moayeri solutions than the others.

8. Results and discussion

To study the effect of upstream face angle α and position of the horizontal filter on seepage characteristics, large numbers of runs were carried out . The present problem was studied with nine values of (α = 10°, 20°,..., 90°), and thirty-one value of (*Xb/Hu* =0, 0.1, 0.2,..., 3.0), producing 278 runs in total. Of course the run corresponding to α = 90°, *Xb*=0 was excluded. Runs carried for α = 90°, can be used to simulate a dam with vertical core and inclined upstream shoulder with high permeability.

Fig. 9 and 10 show free surface profile and relative seepage rates *q/k* along the horizontal filter for (α = 10°, 30°, 60° 90°, and *Xb/Hu* =0,1,2,3. It can be seen that, crossed part of the filter increases as α increases with decreasing rate as *Xb/Hu* increases. Also, for the same angle α, crossed distance, *L*, from the filter decreases as *Xb/Hu* increases. Free surface always meets the drain at 90°. The free surface profile is mainly determined from *Xb/Hu,* and secondary affected by α. Relative seepage rate *q/k* along the filter always ranges from infinity (from mathematical point of view) at the beginning of the filter at point *C* to 1.0 at the end of the filter at point *D*.

Influences of different combinations between (α = 10°, 30° ,60°, 90°) and (*Xb/Hu =0,0.5,1, 1.5,2, 2.5,3*) on relative seepage rate *q/k* crosses the upstream face of the dam is shown in fig. 11. In this figure horizontal axes represent distance along the upstream face measured from point *B* till point *A* for *Hu=1.0m*, see fig. 1. Seepage rate *q* at the tip of the upstream face, point *A*, is always equal to *k. sin* (90°-α). This means that *q* at point *A* decreases with an increasing rate as α increases. At lowest point of the upstream face of the dam, point *B*, *q* equal to zero for α=90°. Minimum quantity of *q* (*qmin*) is always located at point *B* except for α=90°, where *qmin* is located at point *A*. When α equals to 10°, seepage flows only through the upper third of the upstream face. As α increases, seepage starts to percolate lower part of the upstream face with an increasing rate. When α reaches 90°, it can be found that, most of the total quantity of seepage passes through the lower part of the upstream face. Fig. 12-a shows variation in maximum seepage rate (*qumax*) along the upstream face of the dam corresponding to different values of α and *Xb/Hu*. Fig. 12-b shows different relative elevations of *qumax*.

From figs. 12, it can be seen that max. seepage rate *qumax* for α = 10°,20°,30° were found at the top of the upstream face at point *A* with magnitude equal to $k.\sin(90-\alpha)$. As α increases more than 30°, *qumax* starts to increase in magnitude than $k.\sin(90-\alpha)$ and moves down along the upstream face to point *B*. The rate of this behavior increases as *Xb/Hu* decreases. For *Xb/Hu=3.0* qumax is always found at point *A* except for $\alpha = 90^{\circ}$, where *qumax* is always located at the neighborhood node to point *B*.

For all the carried runs the relative differences between inflow and outflow seepage rates was ranged between 0.1% and 1% . Total amount of seepage for any run was assumed to be equal to the average of seepage flow in through the upstream face and out from downstream filter of the dam.

The total amount of seepage flow through the dam and the crossed part of the horizontal filter increase with an increasing rates as α increases and *Xb/Hu* decreases as shown in Figs. 13-a, b, respectively.

The position of the point of inflection on the free surface, if existed, depends upon both variables *Xb/Hu* and α, as shown in fig. 14. The inflection point approaches the top of the upstream face, point *A*, as *Xb/Hu* decreases or as α increases. Broken curves in fig. 14 are due to representing the continues curvature of the free surface profile with linear elements. No inflection points can be appeared for

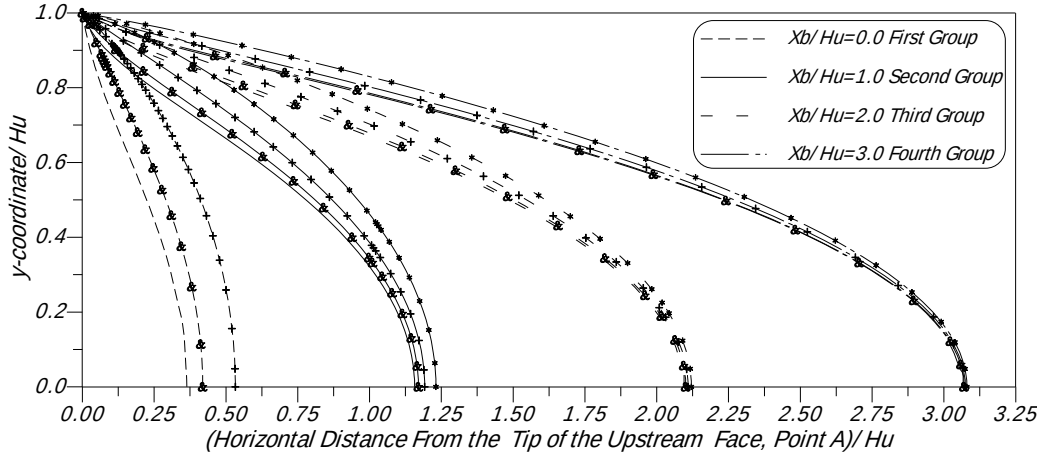

Fig. 9. Comparison between different configurations of the free surface under different combinations of [α°=10 (no symbol), 30 (&), 60(+), 90(*)], and [*Xb/Hu* =0.0, 1.0, 2.0, 3.0].

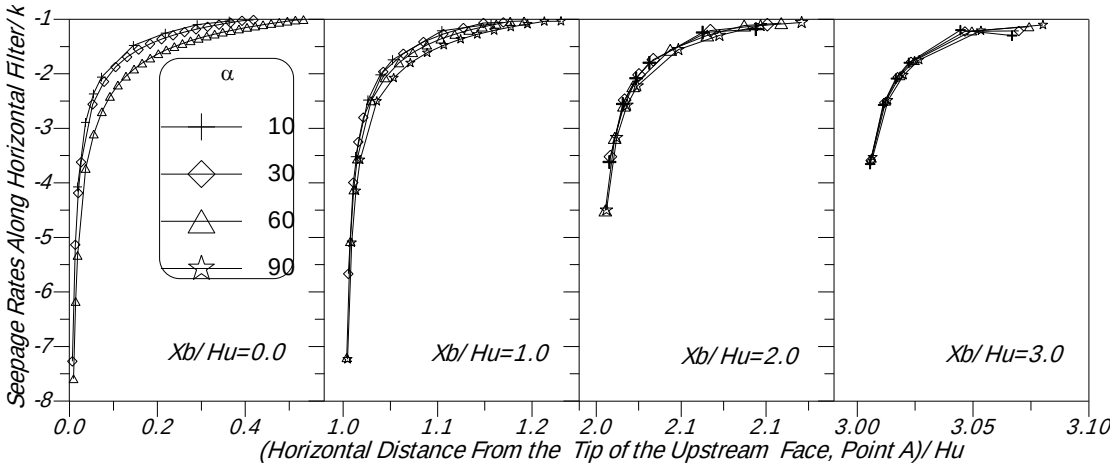

Fig.10. Relative seepage rates along horizontal filters for different values of α° and *Xb/Hu.*

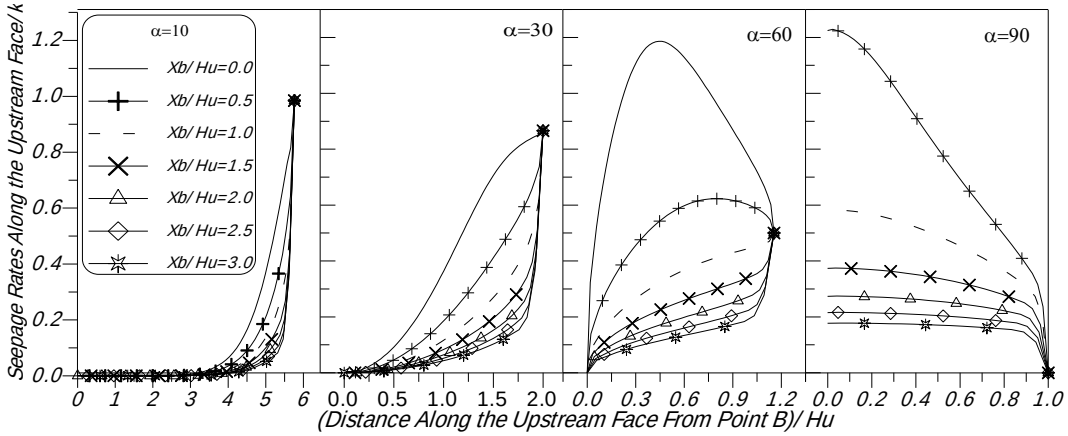

Fig.11. Relative seepage rates along the upstream face of the dam for different values of α° and *Xb/Hu.* (Horizontal axe represents distance along the upstream face).

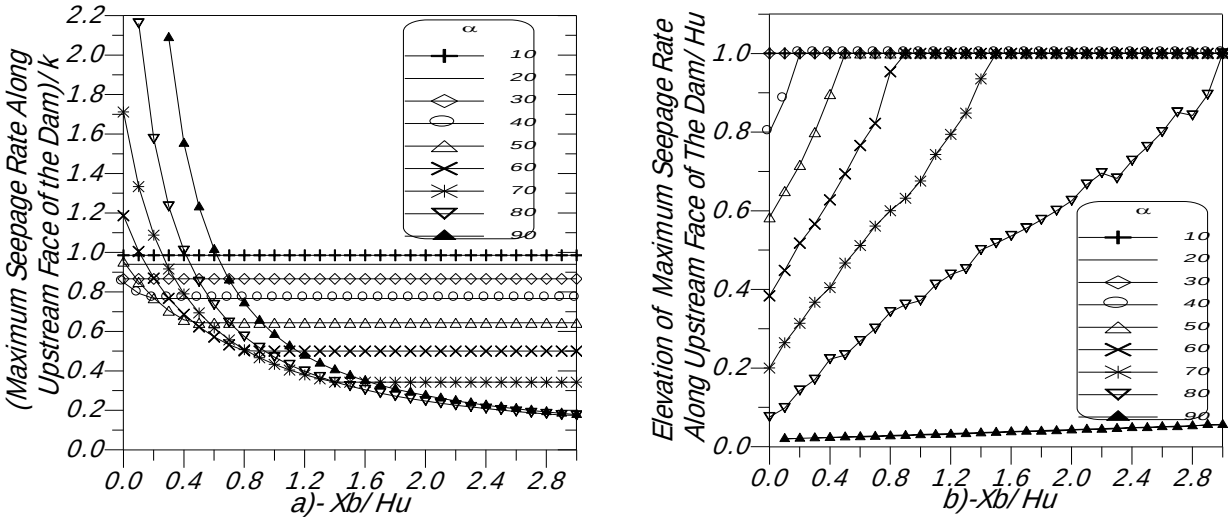

Fig.12-a. Maximum relative seepage rates and b) its relative elevations along the upstream face of the dam for different values of *Xb/Hu* and α .

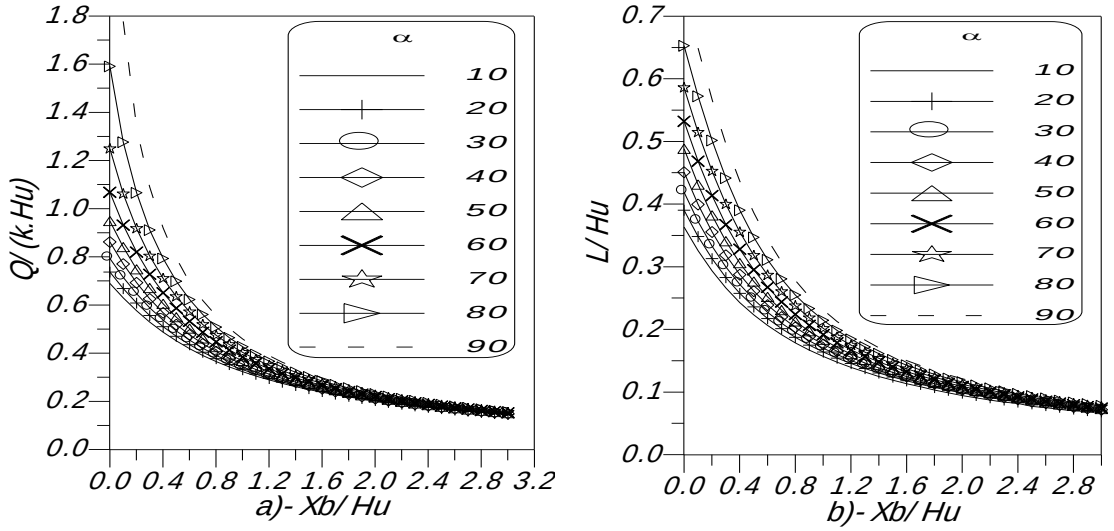

Fig.13. Effect of different values of α and *Xb/Hu* on a) relative total amount of flow through the dam and b) relative crossed length of the horizontal filter.

rectangular dams, $\alpha = 90^{\circ}$. Form figs. 12 and 14 it can be observed that the free surface profile of the flow generate an inflection point only if maximum seepage rate along the up-stream face lies at point *A*.

9. Conclusions and recommendation

Mathematical model based on BEM was developed and used to obtain a numerical solution to the problem of seepage through homogeneous and isotropic earth dams with a horizontal filter. Earth dams with upstream face slope, α, equal to 10°, 20°,...., 90° were considered in combination with different positions of the filter, *Xb/Hu=0, 0.1, 0.2, 0.3,..., 3.0*. The results were given partly in forms of graphs. The following notes can be concluded:

1. Casagrande's method gives good results only when the values of *Xb/Hu* are large than unit.

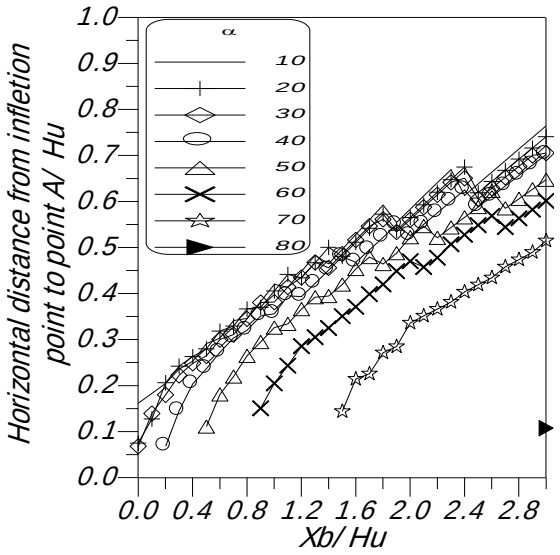

Fig. 14. Effect of different values of and *Xb/Hu* on relative location of the inflictions of the infliction points.

2. Numerical solutions of the BEM are in good agreement with analytical solutions of Moayeri and Numerov.
3. Free surface profile are mainly dependent on *Xb/Hu* and secondly on α .
4. Seepage rates along upstream face of the dam are depended strongly on values of α and *Xb/Hu*.
5. Positions of maximum seepage rate *qumax* along the upstream face of the dam coincide with the highest wetted point on the upstream face for $\alpha \leq 30^{\circ}$ with magnitude equal to $k.sin\ (90^{\circ} - \alpha)$. As α increases, locations of *qumax* move downward to the upstream toe with value higher than $k.sin\ (90^{\circ} - \alpha)$ as *Xb/Hu* decreases.
6. Relative rate of seepage *q/k* along the filter always vary from infinity at the beginning of the filter to 1.0 at its end.
7. Both of total rates of flow through the dam and crossed part of the filter are directly proportional with values α and *Hu/Xb*. But the effect of α diminishes as *Xb/Hu* increases.
8. As α decreases than 90° and *Xb/Hu* increases an inflection point starts to appear along the free surface. The free surface profile always has an inflection point if maximum seepage rate along the upstream face is located at the tip point of the upstream face of the dam, point *A*.

Present problem can be solved accurately using numerical approach as BEM or analytical approach as conformal mapping and inverse hodograph. Analytical solutions ended with complex relations between the desired output and the dependent variables, such relations needs especial skills in mathematics (i.e., elliptic integrals and finding roots of equations) and programming to handle. In the other hand, numerical models need an accurate program to be applied. Thus it's recommended to create accurate and simple formulations between output and input variables of this problem. This will be the scope of the next work.

References

[1] E. Harr, Groundwater and Seepage, McGRaw-Hill Book Company, p. 315 (1962).
[2] M.S. Moayeri, "Seepage Through Dams With Horizontal Toe Drain", Journal of Soil Mechanics and Foundations Division, ASCE, Vol. 98 (SM5), pp. 461-479 (1972).
[3] H.M. Hathoot, "Seepage Through Earth Dam With A Horizontal Toe Filter", The Bulletin of The Faculty of Engineering, Alex. University, pp. 337-349 (1977).
[4] P. Shlomo Neuman and Paul A. Witherspoon, "Finite Element Method of Analyzing Steady Seepage with a Free Surface", Water Resources Research Vol. (3), pp. 889-897 (1970).
[5] A. James Liggett, "Location of Free Surface in Porous Media", Journal of the Hydraulic Division, Vol. 103 (HY4), pp.. 353-365 (1977).
[6] J.S.P. Jaime Cabral and C. Luiz Wrobel, "Unconfined Flow Through Porous Media Using B-Spline Boundary Elements", Journal of Hydraulic Engineering, Vol. 117 (11), pp. 1479-1495 (1991).
[7] F. Abdrabbo, "An Application of the Boundary Element Method to Seepage Problem-II) Unconfined Flow Problem", the Bulletin of the Faculty of Engineering, Alex. University, pp. 495-532 (1985).

[8] C.O. Li and D.V. Griffith, "Finite Element Modeling Of rapid Draw down", Numerical Methods in Geomechanics, G. Swoboda Insbruck (1988).

[9] L. Lam and D.G. Fredlund, "Saturated – Unsaturated Transient Finite Element Seepage Model for Geo-technical Engineering", Proceeding of the 5th International Conference, Burlington, Vermont, U.S.A., pp. 113-122 (1984).

[10] F. Paris and J. Canas, Boundary Element Method Fundamentals and Applications, Oxford University Express, p.392 (1997).

[11] J.A. Liggett, and P.L-F. Liu, "The Boundary Integral Equation Method For Porous Media Flow," George Allen & Unwin, p. 255 (1983).

Received January 15, 2004
Accepted July 12, 2004